Proceedings of the American Control Conference
San Diego, California • June 1999

Model Reduction and Design of a Power Steering System

Âli Yurdun Orbak, Kamal Youcef-Toumi and Masaaki Senga
Department of Mechanical Engineering

Massachusetts Institute of Technology
Cambridge, MA 02139

Abstract

In control system analysis, there is an increasing need for obtaining low order approximations of high order models of physical systems. Low order models result in several advantages including the reduction of computational complexity and improved understanding of the original system structure. This topic has been studied for many years now, and many methods have been suggested for obtaining suitable low order approximations. In a previous work [1], a new physical domain model reduction procedure was presented. In this paper, this new model reduction procedure will be applied to a power steering system. The usefullness of the procedure will be investigated from a design point of view.

1. Introduction

In a previous work [1], a decomposition procedure for physical systems was introduced as a basis for a new model reduction procedure. The decomposition procedure is based on local loop gains of bond graphs which helps the user to identify the modes of a physical system. Once the components or subsystems are identified, they are ordered according to their importance by using information from residues [2].

In this paper, the same idea will be applied to a real engineering system, namely a power steering system. With this application, we will also show how this new model reduction procedure can be used in design of engineering systems.

A power steering system, shown in Figure 1, consists of two main units, namely a manual power transfer unit and a power assist unit. The manual unit consists of a steering wheel, a main shaft and a gear mechanism.

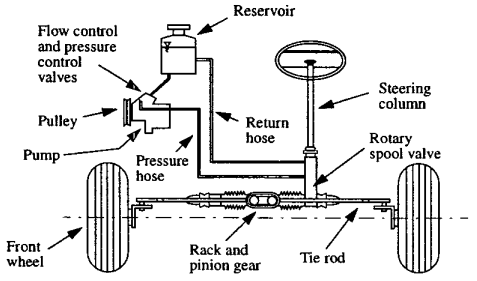

Figure 1: A power steering system.

0-7803-4990-6/99 $10.00 © 1999 AACC

There are two types of power steering systems: namely hydraulic power steering system and electric power steering system. An electric power steering system is more convenient than a hydraulic power steering system because of its ease of use. However, because of size, reliability and safety reasons hydraulic power is preferred at this time. In this paper, a hydraulic power steering system will be used. The main parts of a hydraulic power steering system are: an oil pump, hoses and pipes, an oil reservoir, a steering wheel, a main shaft, steering gear box that contains a pressure control valve, a rack and pinion gear mechanism, a piston and power cylinder. Steering torque from the driver is transferred from the steering wheel to the pinion gear. The pressure control valve is placed between the main shaft and the pinion gear, so that the valve moves corresponding to the input torque. The valve displacement from the neutral position produces an oil pressure change, and the pressure is guided to one of the cylinders corresponding to the valve movement direction. The pressure is converted to the force by the piston attached to the rack bar, and the force assists the driver to steer the front wheels.

2. Power steering system model

A bond graph model of this system can be seen in Figure 2. The variables are defined as in Tables 1 to 3 and the values of system parameters can be seen in Tables 4 to 6. The details and formulation of this bond graph model can be found in [3]. It can be seen from the bond graph that this system is of order 9. Assumptions behind this model are: (1) Mass of the oil in a pipe is treated as inertance, (2) pressure drop associated with a pipe is treated as resistance, (3) compressibility of the oil in a pipe is treated as capacitance, (4) expandability of the hose is treated as capacitance, (5) mass of the oil in a hose is included in the mass of the oil in a pipe, (6) compressibility of the oil in a hose is included in the hose expandability, and (7) pressure drop associated with a hose is included in the pipe resistance.

Here, the nine states are:

$$\begin{pmatrix} \text{pressure at pump outlet port} \\ \text{flow rate through pipe \# 1} \\ \text{pressure in hose \# 1} \\ \text{flow rate through pipe \# 2} \\ \text{pressure in hose \# 2} \\ \text{flow rate through pipe \# 3} \\ \text{rack bar velocity} \\ \text{load spring force} \\ \text{torsion bar torque} \end{pmatrix} = \begin{pmatrix} P_p \\ Q_{P12} \\ P_{H1} \\ Q_{P2} \\ P_{H2} \\ Q_{P3} \\ \dot{x}_L \\ F_L \\ \tau_L \end{pmatrix} \quad (1)$$

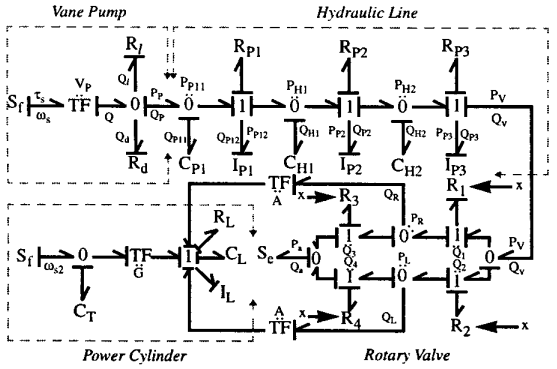

Figure 2: A bond graph model of the power steering system.

and the inputs are:

$$\begin{pmatrix} \text{pump output flow rate} \\ \text{steering wheel angular velocity} \end{pmatrix} = \begin{pmatrix} Q_P \\ \omega_{s2} \end{pmatrix} \tag{2}$$

For our purpose, we linearized this nonlinear system about its operating point. The details of this linearization can be found in [3]. This concludes our introduction of the physical system. As one can see this is a multi-energy domain system. Experimental and simulation results indicated that this system has high oscillations. It had been concluded [3] that these vibrations come from the hydraulic line. Now, we will show how a decomposition procedure [1] can help in obtaining a reduced order model and detecting this phenomenon.

3. Model reduction

If we closely examine the system, we see that the only part that can be reduced is the hydraulic line, as it might contain hose and pipe capacitances and inertances that have less impact on the system behavior. The bond graph representation of this hydraulic line is shown in Figure 3. Here, R_V represents the effective resistance of the rotary valve. If the line is open to air $R_V = 0\ \frac{N\,sec}{m^5}$ and if the rotary valve is almost closed $R_V = 2 \times 10^9\ \frac{N\,sec}{m^5}$. In this paper we will use $R_V = 0\ \frac{N\,sec}{m^5}$.

The hydraulic line is of order 6. This line model is reduced by using the procedure of [1]. Using $\mathbf{x} =$ $[P_P\ Q_{P12}\ P_{H1}\ Q_{P2}\ P_{H2}\ Q_{P3}]^T$ as the state vector, the state-space equations of this line can be written as,

$$\dot{\mathbf{x}} = \mathbf{A}\mathbf{x} + \mathbf{B}u \tag{3}$$

where

$$\mathbf{A} = \begin{bmatrix} 0 & -\frac{1}{C_{P1}} & 0 & 0 & 0 & 0 \\ \frac{1}{I_{P1}} & -\frac{R_{P1}}{I_{P1}} & -\frac{1}{I_{P1}} & 0 & 0 & 0 \\ 0 & \frac{1}{C_{H1}} & 0 & -\frac{1}{C_{H1}} & 0 & 0 \\ 0 & 0 & \frac{1}{I_{P2}} & -\frac{R_{P2}}{I_{P2}} & -\frac{1}{I_{P2}} & 0 \\ 0 & 0 & 0 & \frac{1}{C_{H2}} & 0 & -\frac{1}{C_{H2}} \\ 0 & 0 & 0 & 0 & \frac{1}{I_{P3}} & -\frac{R_{P3}+R_V}{I_{P3}} \end{bmatrix}$$

and

$$\mathbf{B} = \begin{bmatrix} \frac{1}{C_{P1}} & 0 & 0 & 0 & 0 & 0 \end{bmatrix}^T$$

In this case, we are interested in the pressure P_P, so

$$y = P_P = \begin{bmatrix} 1 & 0 & 0 & 0 & 0 & 0 \end{bmatrix} \mathbf{x} = \mathbf{C}\mathbf{x} \tag{4}$$

One can now calculate the loop gains and local damping ratios using the numerical values listed in Tables 4 and 5

Table 1: Table for the important variables in bond graph representation.

$K_T = \frac{1}{C_T}$	Torsion bar spring constant
G	Gear ratio
R_L	Resistance of the load
C_L	Capacitance of the load
I_L	Inertance of the load
P_V	Pressure at the valve inlet port
Q_V	Flow rate from the hydraulic line
ω_{s2}	Steering wheel angular velocity

Table 2: Table for the important variables in bond graph representation.

Variable	Detailed name of the variable
ω_s	Pump shaft angular velocity
τ_s	Torque developed at the driven shaft
V_P	Geometric displacement per radian rotation of the pump
Q_l	Pump leakage flow rate
Q_d	Pump discharge flow rate
Q_P	Actual pump flow rate to the outer system
P_P	Back pressure determined by the outer system (or pressure at the pump outlet port)
Q_n	Flow rate that goes through the orifices, $n = 1 \ldots 4$
P_a	Ambient pressure
Q_a	Flow rate into the tank
P_R	Pressure at the right cylinder
P_L	Pressure at the left cylinder
Q_R	Flow rate into the right cylinder
Q_L	Flow rate into the left cylinder
x	Spool displacement that modulates the orifice resistance

Table 3: Table for the important variables in bond graph representation.

R_l	Resistance associated with the internal pump leakage
R_d	Resistance associated with the relief valve
R_n	Resistance corresponding to the valve orifice, $n = 1 \ldots 4$
R_{Pn}	Resistance associated with the n'th pipe, $n = 1 \ldots 3$. Calculated by: $R_{Pn} = \frac{128\,\mu\,l_{Pn}}{A_n}$.
I_{Pn}	Inertance associated with the n'th pipe, $n = 1 \ldots 3$. Calculated by: $I_{Pn} = \frac{\rho\,l_{Pn}}{A_n}$.
C_{Pn}	Capacitance associated with the n'th pipe, $n = 1 \ldots 3$. Calculated by: $C_{Pn} = \frac{A\,l_{Pn}}{K}$.
C_{Hn}	Capacitance associated with the n'th hose, $n = 1 \ldots 2$. Calculated by: $C_{Hn} = k\,l_{Hn}$.

Table 4: Parameter values for pipes.

Pipe #	l_P [m]	I_P [$\frac{kg}{m^4}$]	R_P [$\frac{N\,sec}{m^5}$]	C_P [$\frac{m^5}{N}$]
1	1.369×10^{-1}	1.45×10^{6}	5.30×10^{6}	6.72×10^{-15}
2	3.687×10^{-1}	3.90×10^{6}	1.43×10^{7}	1.81×10^{-14}
3	7.8×10^{-2}	8.24×10^{5}	3.02×10^{6}	3.83×10^{-15}

Table 5: Parameter values for hoses.

Hose #	l_H [m]	C_H [$\frac{m^5}{N}$]
1	4.546×10^{-1}	1.67×10^{-12}
2	2.183×10^{-1}	8.0×10^{-13}

as: $\frac{1}{C_{P1}I_{P1}} = 102.63 \times 10^6$, $\frac{1}{I_{P1}C_{H1}} = 0.413 \times 10^6$, $\frac{1}{I_{P2}C_{H1}} = 0.15354 \times 10^6$, $\frac{1}{I_{P2}C_{H2}} = 0.3205 \times 10^6$, $\frac{1}{C_{H2}I_{P3}} = 1.517 \times 10^6$. And $\frac{R_{P1}}{2\sqrt{I_{P1}/C_{P1}}} = 1.804 \times 10^{-4}$, $\frac{R_{P1}}{2\sqrt{I_{P1}/C_{H1}}} = 2.844 \times 10^{-3}$, $\frac{R_{P2}}{2\sqrt{I_{P2}/C_{H1}}} = 4.6787 \times 10^{-3}$, $\frac{R_{P2}}{2\sqrt{I_{P2}/C_{H2}}} = 4.8709 \times 10^{-4}$, $\frac{R_{P3}}{2\sqrt{I_{P2}/C_{H2}}} = 6.8389 \times 10^{-4}$, $\frac{R_{P3}}{2\sqrt{I_{P3}/C_{H2}}} = 1.4878 \times 10^{-3}$. Table 7 shows the residues, absolute values of the residues and the corresponding eigenvalues.

This table suggests that the first complex mode is the most important one and it should be retained in a reduced order model. Indeed, when we look at the numerical values of the loop gains and the local damping ratios calculated above, we see that this hydraulic line can be seperated into three subsystems. The first subsystem consists of I_{P1}, C_{P1} and R_{P1} (a second order system), the second subsystem consists of I_{P2}, C_{H1}, R_{P2} and the third subsystem consists of I_{P3}, C_{H2}, R_{P3}. The eigenvalues of the first subsystem are $-1.8276 \pm 1.0131 \times 10^4 i$ which are close to the dominant complex poles of the hydraulic line. As a result we can reduce this hydraulic line from order 6 to order 2 by taking the first subsystem as the reduced order model. Time and frequency responses of this system for a step input of $Q_P = 1 \times 10^{-4}\ \frac{m^3}{sec}$ can be seen in Figure 4. These results are acceptable for this system. One can also see a frequency difference in the response of Figure 4(a). This occurs as a result of a 20 $\frac{rad}{sec}$ difference in original and reduced order model eigenvalues ($\approx 10151 - 10131 = 20$). In addition, a steady-state error (DC gain difference) exists.

One can also see that this first subsystem, which is also the reduced order model, gives the highest vibration mode. So now, we can understand the nature of this vibration of the steering system and try to prevent or reduce it to acceptable limits by changing its dynamic characteristics. In the next subsection we will explore these design issues.

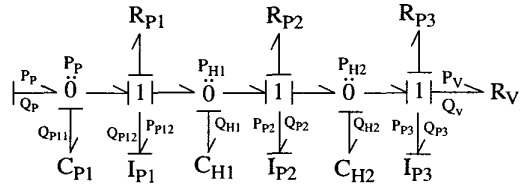

Figure 3: Hydraulic line of the power steering system.

Table 6: Other necessary parameter values.

Parameter	Value
ω_s	52.4 $\frac{rad}{sec}$
ω_{s2}	$\frac{\pi}{2} sin 2\pi t$
R_l	$5.504 \times 10^7\ \frac{kg^{1/2}}{m^{7/2}}$
R_d	$2.420 \times 10^7\ \frac{N\,s}{m^5}$
$K_T = \frac{1}{C_T}$	92.8 $\frac{N\,m}{rad}$
G	127.7 $\frac{m}{rad}$
R_L	$2.72 \times 10^4\ \frac{N\,s}{m}$
C_L	$1 \times 10^{-6}\ \frac{m}{N}$
I_L	50 kg
A, piston area	$1.0 \times 10^{-3}\ m^2$
A_n, cross section area of pipes, $n = 1 \ldots 4$	$7.85 \times 10^{-5}\ m^2$
d_n, pipe diameters, $n = 1 \ldots 4$	10 mm
k, hose expandability	$2.7248 \times 10^{11}\ \frac{N}{m^4}$
l_v, orifice groove length	15 mm
r, valve body radius	10.5 mm
b, length of the valve underlap at the neutral position	0.1975 mm
K, oil bulk modulus	$1.6 \times 10^9\ \frac{N}{m^2}$
ρ, oil density	$0.83 \times 10^3\ \frac{kg}{m^3}$
μ, oil viscosity	$0.95 \times 10^{-2}\ \frac{N\,sec}{m^2}$

Table 7: Table for the residues, their absolute values, and the corresponding eigenvalues of the hydraulic line.

Residue	Absolute value of the residue	Eigenvalue
$7.4106 \times 10^{13} \mp 1.3342 \times 10^{10} i$	7.4106×10^{13}	$-1.8276 \pm 1.0151 \times 10^4 i$
$5.0804 \times 10^{9} \mp 6.8041 \times 10^{6} i$	5.0804×10^{9}	$-1.8327 \pm 1.3661 \times 10^3 i$
$2.9401 \times 10^{11} \mp 1.5287 \times 10^{9} i$	2.9402×10^{11}	$-1.8332 \pm 3.5258 \times 10^2 i$

4. Design issues for the hydraulic line

In the previous section, we concluded that the undesirable vibrations with the highest frequency and amplitude originates from the first pipe of the hydraulic line. Now we will change the hydraulic line characteristics to decrease the vibrations.

4.1. Characteristics of the hydraulic line components

The hydraulic line of the power steering system that we discussed in the previous section consists of two hoses and three pipes (see the schematic in Figure 5).

Hoses are composed of three elements: inner tube, reinforcement and cover. Hose reinforcement surrounds an inner tube and its material is usually fabric, cord or metal layers. These elements give strength to the hose against the internal pressure and external forces. Pipes, on the other hand, are made up of various materials such as steel, copper, brass, aluminum, stainless steel and plastic. Hydraulic power steering systems usually use brass pipes.

With the assumptions described earlier, the approximation of the parameter values are derived as follows. The flow in a pipe has a Reynolds number of 873.7 (less than 2000) which indicates that the flow is laminar. So we can

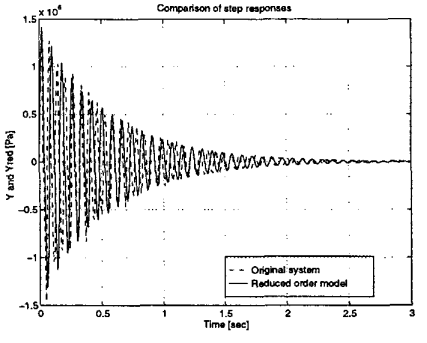

(a) Comparison of time responses.

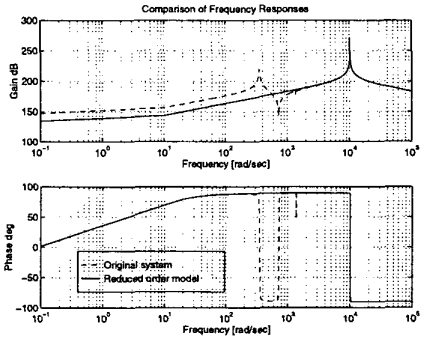

(b) Comparison of frequency responses.

Figure 4: Comparison of responses of the hydraulic line.

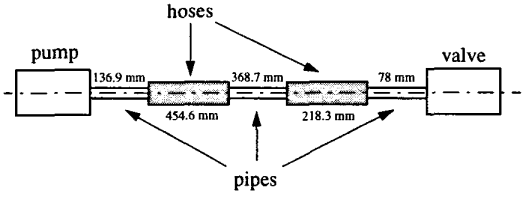

Figure 5: Hydraulic line schematic of the power steering system.

use Hagen-Poiselle's equation to get the pipe resistance,

$$P_{\text{in}} - P_{\text{out}} = \frac{128\mu l_P}{\pi d^4} Q \tag{5}$$

For the pipe inertance, one can consider a force balance,

$$\frac{dv}{dt} A\rho l_P = A(P_{\text{in}} - P_{\text{out}}) \quad ; \quad Q = vA \tag{6}$$

Assuming linear relationship for pipe and hose capacitances we can write,

$$\frac{Al_P}{K}\frac{dP}{dt} = Q_{\text{in}} - Q_{\text{out}} \tag{7}$$

and

$$kl_H \frac{dP}{dt} = Q_{\text{in}} - Q_{\text{out}} \tag{8}$$

As a result, the following parameters are calculated for design[1]:

$$\left.\begin{aligned} I_P &= \frac{\rho l_P}{A} \\ C_P &= \frac{Al_P}{K} \\ R_P &= \frac{128\mu l_P}{\pi d^4} \\ C_H &= kl_H \end{aligned}\right\} \tag{9}$$

Tables 4 through 6 show the necessary numerical values. This completes our discussion on the parameter values. Now let's discuss how we can decrease the high frequency vibration by design.

According to our structural analysis, we already know that the highest frequency is coming from the first pipe (I_{P1}, C_{P1}, R_{P1}). Therefore, this vibration can be reduced by changing these parameters. If one looks at the dynamic behavior of the hydraulic line, he/she sees that in this case, in order to reduce the vibration, the pipe resistance, R_{P1}, needs to be increased. This parameter is directly related to the length, so we should change the length of the pipe to get a reduced vibration frequency. On the other hand, there is a physical limit on this length and we cannot change it to any value. The total length of the hydraulic line cannot be shorter than the distance between the pump and the valve[2]. Also, because of heat and other problems such as connecting to the main frame or to other parts, it should not be longer than, for instance, $1.50\,m$.

A feasible way to achieve this design is to double the length of the first pipe without changing its remaining current physical characteristics. If we double the length and use a brass pipe of approximately $28\,cm$, maximum vibration frequency is reduced to 792.6 Hz, which is less than half of the original frequency value. One should also keep in mind that changing the length of the first pipe, changes all the related parameters of this pipe (I_{P1}, C_{P1} and R_{P1}), but the changes work in our favor. By the length increase we get a lower frequency vibration as the damping ratio increases. By this increase, the total length of the hydraulic line becomes $1.40\,m$ which is less than our limiting length. Another way of changing this resistance may be to change the oil that is used, but this is usually not a preferred option because of its expense[3].

As a second design point, the second vibration mode frequency, that is introduced from the second subsystem (I_{P2}, R_{P2} and C_{H1}), can also be reduced by decreasing the hose stiffness. And hose stiffness can again be changed by the length of the hose or by changing the hose material (and consequently changing the expandability coefficient). As we have already increased the length of the first pipe and still have some more space, we can change the length of this hose. But we might face with space problems by changing all the lengths of hoses and pipes. So, the easiest design approach in this case will be to change the material inserts or restrictors and consequently change the hose expandability coefficient. There are many available hoses that can be used which can decrease the hose stiffness about 10000 times to

[1] Here A represents the cross section area of the pipe.

[2] For this system, the minimum distance is approximately 95 cm.

[3] Companies usually try to use the same material that they used in their previous designs, to cut extra costs.

decrease the vibration frequency to a very low value. Note that changing the hose expandability is a much efficient way than changing the length as we need to increase the length of the hose too much to get the same stiffness value. Again the vibration decreases as the damping ratio increases. The results of frequency response simulation with both of these changes at the same time can be seen in Figure 6.

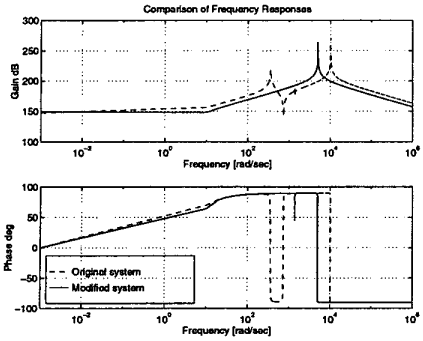

Figure 6: Comparison of frequency response simulations of the original and modified model of the hydraulic line (modification is by parameter changes).

In these plots one can detect that, although the vibration frequency of the first mode has been reduced, the high peak is still present. In order to decrease or totally eliminate this peak we need to somehow further increase the damping of the system. If we return to the bond graph of the hydraulic line, we conclude that, adding a dissipation element in series (adding to the first **1** junction, see Figure 7), we can increase the damping. The simulation results with this modification indicates that if we use a lower value, for the dissipation (such as $R_{added} = 5 \times 10^9 \frac{N\,sec}{m^5}$), one can still notice a slight peak at the same frequency value. But as we increase the parameter value (to $R_{added} = 2 \times 10^{10} \frac{N\,sec}{m^5}$, as in Figure 8), the peak can totally be eliminated. Note that, in this simulation the second mode of vibration has already been eliminated by the hose modification but the first pipe length has not been changed. One should notice that adding dissipation elements to other hoses or pipes in series will not effect this first mode, and this information was obtained using the new model reduction algorithm.

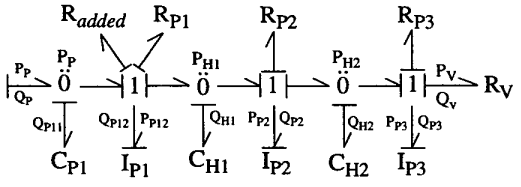

Figure 7: Modified hydraulic line of the power steering system.

In this subsection, we discussed how we can change the design parameters of the hydraulic line to prevent undesirable high vibrations using the results of our new model reduction procedure[4]. The new procedure identifies the system subsystems that give certain system behavior (in this case the high frequency vibration that is dominated by the dynamics of the hydraulic line). Consequently, by changing the characteristics of contributing subsystem parameters we can redesign the system to prevent this vibration.

[4]In this particular example, the new procedure was used to identify the system structure rather than actually reducing the model order.

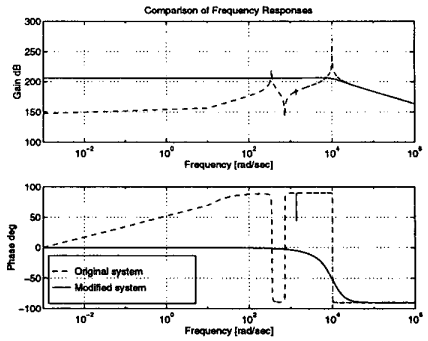

Figure 8: Comparison of frequency response simulations of the original and modified model of the hydraulic line (modification is by adding a dissipation element in series).

5. Steady-state considerations

As we know, steady-state response is the behavior of the system outputs as time approaches infinity. The steady-state solution of dynamic systems with constant inputs is also often of interest. As we saw in previous section, when the new model reduction procedure is used, we might have steady-state error (DC gain difference), if we are eliminating some components without adding their effects to elsewhere (or combining them with other parameters/components appropriately). Basically, this error can be compensated by one of the three approaches: (1) By adding a gain[5] to the reduced order model with a numerical value of $\frac{y_{ss}}{y_{red_{ss}}}$, (2) By increasing the order of the reduced order system (with increasing the number of subsystems retained), (3) By computing the steady-state error, and then modifying the reduced order model accordingly.

Here, we will show, how we can employ bond graphs to obtain information about steady-state and refine our reduced order models accordingly and apply this approach to the hydraulic line of the power steering system.

5.1. Calculating steady-state error from bond graphs

It is well known that, one way of calculating the steady-state values is the use of algebra. Namely, at steady-state, $\dot{\mathbf{x}} = 0$, then

$$\dot{\mathbf{x}} = \mathbf{A}\mathbf{x} + \mathbf{B}\mathbf{u} \quad \Rightarrow \quad \mathbf{x}_{ss} = -\mathbf{A}^{-1}\mathbf{B}\mathbf{u}_{ss} \tag{10}$$

and[6]

$$\mathbf{y} = \mathbf{C}\mathbf{x} \quad \Rightarrow \quad \mathbf{y}_{ss} = \mathbf{C}\mathbf{x}_{ss} \tag{11}$$

When $\mathbf{A}$ is singular, $\mathbf{x}_{ss}$ cannot be calculated by equation (10). As a result, we cannot see which parameters are responsible for the steady-state solution.

[5]This can lead to incorrect results in the transition region of the simulation.

[6]Here, $\mathbf{u}_{ss}$ is the constant value of the input at steady-state, i.e. if the input is a step, then this step value will be $\mathbf{u}_{ss}$.

In order to eliminate such problems and to get more information from the system structure, we can use a procedure on bond graphs to get the steady-state solution, just by solving a set of algebraic equations [4]. In this paper, we will present a slightly different algorithm then [4] to obtain the steady-state solution:

1. Complete causality assignment on the bond graph,
2. Remove energy storage elements with derivative causality,
3. Replace remaining energy storage elements by sources with the same causality (i.e. $C \rightarrow S_e$ and $I \rightarrow S_f$),
4. Write down new junction equations,
5. Set output of newly added sources to zero and solve for their inputs. These values will be the steady-state values of their coresponding states[7].

This method also reveals important information about the system structure, and it can be applied to both SISO and MIMO systems. Now we will briefly go over the hydraulic line of the power steering system, while keeping in mind the discussion above.

5.2. Hydraulic line of the power steering system

The modified bond graph representation of the hydraulic line with the discussion on steady-state can be seen in Figure 9.

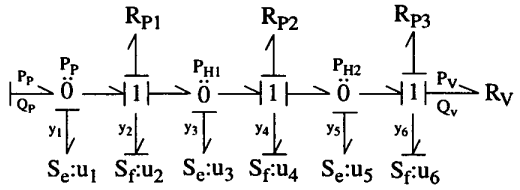

Figure 9: Modified representation of the hydraulic line.

The calculations can be written as:

$$\begin{aligned} y_1 &= Q_P - u_2 \\ y_2 &= u_1 - R_{P1}u_2 - u_3 \\ y_3 &= u_2 - u_4 \\ y_4 &= u_3 - R_{P2}u_4 - u_5 \\ y_5 &= u_4 - u_6 \\ y_6 &= u_5 - R_{P3}u_6 \end{aligned} \tag{12}$$

Setting $y_1 = y_2 = y_3 = y_4 = y_5 = y_6 = 0$ and solving for u_i leads to:

$$\begin{aligned} Q_{P12_{ss}} &= Q_{P2_{ss}} = Q_{P3_{ss}} = Q_P \\ P_{H1_{ss}} &= P_{P_{ss}} - R_{P1}Q_P \\ P_{H2_{ss}} &= P_{P_{ss}} - (R_{P1} + R_{P2})Q_P \\ Q_{P3_{ss}} &= \frac{P_{H2_{ss}}}{R_{P3}} = Q_P \\ \Rightarrow \quad P_{P_{ss}} &= (R_{P1} + R_{P2} + R_{P3})Q_P \end{aligned} \tag{13}$$

As one can see, the steady-state value of P_P is effected by the sum of all resistances. So, if we add R_{P1}, R_{P2} and R_{P3} together to our second order reduced model, we eliminate the steady-state error. The simulation results can be seen in Figure 10. In Figure 10-(a), one can see the effect of increased damping, and the compensation for the steady-state error (DC gain difference).

[7]This algorithm is similar to setting the derivatives of the states to zero, in order to calculate the steady-state values.

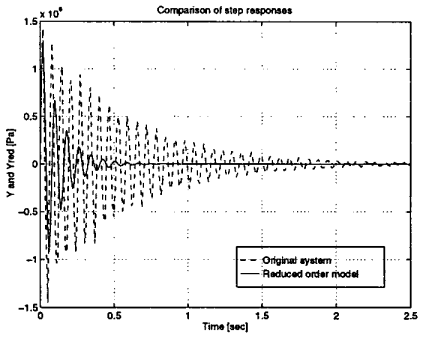

(a) Comparison of step responses.

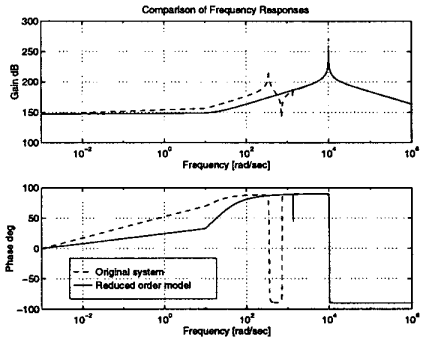

(b) Comparison of Bode plots.

Figure 10: Comparison of full order and 2nd order reduced model of the hydraulic line with modification according to steady-state information.

6. Conclusion

In this paper, we presented an application of the physical domain model reduction to real engineering systems, and showed how it can be used in the design process. The results indicate that this new model reduction procedure is very useful, in the sense that it gives the engineer a better understanding of the original system structure.

References

[1] ORBAK, ÂLI YURDUN and KAMAL YOUCEF-TOUMI. Model reduction in the physical domain. *MIT Report. Department of Mechanical Engineering*, 1998.

[2] ORBAK, ÂLI YURDUN. Physical domain model reduction for design and control of engineering systems. Mech.E. thesis, Massachusetts Institute of Technology, Mechanical Engineering Department, June 1998.

[3] SENGA, MASAAKI. Modeling and analysis of power steering systems. Mechanical engineer's thesis, Massachusetts Institute of Technology, Mechanical Engineering Department, January 1995.

[4] GAWTHROP, P. J. and L. SMITH. Causal augmentation of Bond graphs with algebraic loops. *Journal of the Franklin Institute*, 329(2):291–303, 1992.